Furfuryl Alcohol Polymerization in H−Y Confined Spaces: Reaction Mechanism and Structure of Carbocationic Intermediates

S. Bertarione, F. Bonino, F. Cesano, A. Damin, D. Scarano, and A. Zecchina*

Department of Inorganic, Physical and Materials Chemistry, NIS Centre of Excellence, and Centre of Reference INSTM, University of Turin, Via P. Giuria 7, I-10125 Torino, Italy

Received: May 22, 2007; In Final Form: November 6, 2007

The acid-catalyzed polymerization and resinification, in the 300−673 K interval, of furfuryl alcohol adsorbed in the framework of a protonic Y zeolite is studied by means of FTIR, Raman, and UV−vis spectroscopies. The idea is that restricted spaces can impose a constraint to the growth of the oligomeric chains, therefore moderating the formation of conjugated sequences responsible for the color of the products and allowing their observation by means of spectroscopic techniques. The detailed study of the evolution of UV−vis, FTIR, and Raman spectra upon dosed amount, contact time, and temperature has allowed the spectroscopic features of some of the single species, either neutral and positively charged (carbocationic intermediates), to be singled out and assigned to understand the mechanism of initiation. The vibrational assignments have been confirmed by computer simulations on model compounds and compared with the results of the mechanistic description of the reaction mechanism made in the past (Choura, et al. *Macromolecules* **1996**, *29*, 3839−3850). The spectroscopic methods have been applied in a large temperature range in order to follow also the formation of more complex products into the pores, associated with longer conjugated sequences, gradually filling the open spaces of the zeolite. For samples contacted with furfuryl alcohol at 673 K, this methodology gives information also on the incipient carbonization process, leading to the formation of a carbonaceous replica phase inside the internal porosity of the zeolite.

1. Introduction

Carbonaceous materials derived from polymerization and resinification of furfuryl alcohol have found a useful range of applications in the production of corrosion-resistant materials, of low flammable and low smoke production composites, pastes and agglutinants, electrode materials, and adsorbent materials for methane and hydrogen storage.[1−12]

Acid-catalyzed oligomerization and resinification have been studied intensively in the past, and in general terms, the features of the process are understood. However, many aspects of the process, including the initiation mechanism, are still unknown. For sake of simplicity, we can consider the processes of oligomerization and resinification as separate, the first one occurring at low temperature and the second one becoming predominant at higher values. We shall see in the following that this assumption is not completely valid because there is no clear-cut difference between the two processes and that partial resinification occurs already during oligomerization.

Coming now to the acid-catalyzed oligomerization, Dunlop and Peters,[1] have hypothesized two main mechanisms for the initiation of the process (see Schemes 1 and 2):

(1) The oligomerization occurs via a condensation reaction between the OH of the methylol group of one furan ring and the 5-position of another furan ring, leading to water elimination and formation of a methylene linkage (Scheme 1). This process can continue and lead to the formation of long oligomeric chains.

(2) The condensation reaction occurs between the OH of the methylol group of one furan ring and the methylol group of another furan ring to form a dimethylene ether linkage (Scheme 2). This mechanism can explain the formation of dimeric species but not the polymeric ones.

Of course, if these two mechanisms are simultaneously operating, long linear chains containing both types of bridges can be present in the final product. In fact, the oligomers formed during the process following Scheme 1 can, in principle, react

SCHEME 1: Condensation Reaction between the OH of the Methylol Group of One Furan Ring and the 5-Position of Another Furan Ring to Form a Methylene Linkage

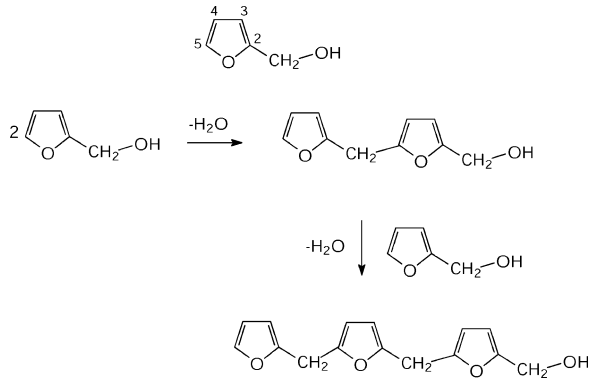

SCHEME 2: Condensation Reaction between the OH of the Methylol Group of One Furan Ring and the Methylol Group of Another Furan Ring to Form a Dimethylene Ether Linkage

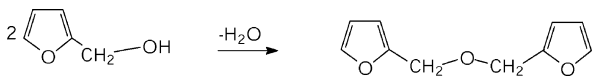

* Corresponding author. Phone: +39 011 6707860. Fax: +39 011 6707855. E-mail: adriano.zecchina@unito.it.

10.1021/jp073958q CCC: $40.75
Published on Web 02/12/2008

SCHEME 3: Formation Reaction of Conjugated Sequences in the Polymer Chains

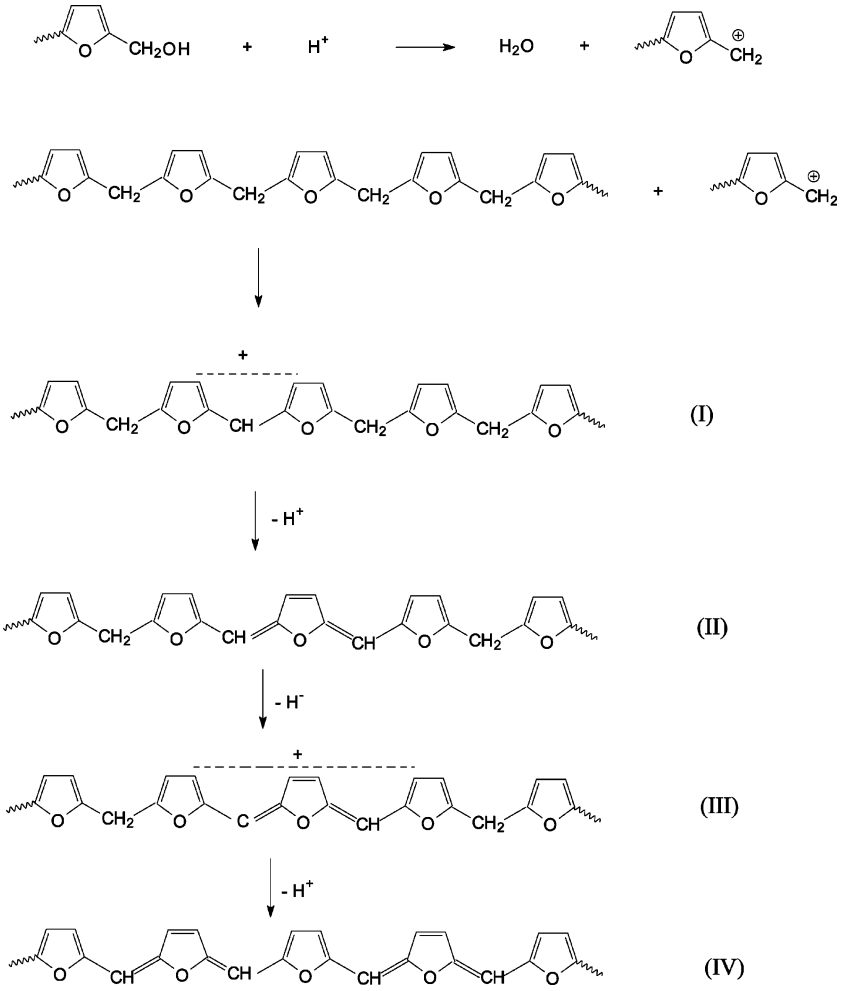

with the monomer following Scheme 2 and give a species containing mixed bridges. The same can in principle be said for the dimeric species formed following Scheme 2, which can further react with monomer to form new species containing mixed bridges.

These pathways and the resulting structures predict only linear macromolecules without any chromophore, and therefore, these materials are expected to be colorless. This prediction is completely different from the experimental observations, since the reacting systems not only become more and more viscous (as expected for a polymerizing system) but develop an intense color too. It is therefore obvious that other reactions producing colored species must accompany the condensation steps and that these "side" events must occur whatever the experimental conditions.

The formation of colored species, being necessarily associated with formation of conjugated double bond sequences, has troubled many researchers in the past, and many attempts to unravel these structures have been published together with proposals of specific mechanisms.[13−17]

The most widely accepted mechanism has been advanced by Gandini et al.[17] These authors have proposed that the formation of conjugated sequences in the polymer chains occurs as reported in Scheme 3.

They proved their hypothesis on the origin of conjugated sequences through the extensive comparison with the properties of model compounds. Following Scheme 3, the oligomers, produced following the mechanism depicted in Scheme 1, undergo hydride-ion exchanges from the carbon atom joining two furan rings with the carbenium ion, formed by water elimination from a protonated methylol termination of another polymer. Notice that in this mechanism the involvement of the H3 and H4 positions in the color-forming mechanism is excluded. It must be emphasized that the first, second, third, and so forth, formed methyl groups are accompanied by the formation of carbenium ions containing 2, 3, 4, and so forth, conjugated rings in positively charged oligomeric species.

The reaction depicted in Scheme 3 can be considered as a side reaction which is introducing sequences of conjugated species inside predominant segments constituted by fully saturated polymeric chains, formed following mechanism 1. Of course, methyl groups and sequences of unsaturated species could be located on the same chain.

It must be mentioned that the side reaction leading to colored species is not the only one occurring during the process. In fact, Conley et al.[15] have suggested that, during the polymerization, the protonic species can attack the oxygen atoms of the furan ring with ring opening and formation of γ-diketone structures (Scheme 4).

However, it must be mentioned that this side reaction is not able to explain the formation of colored species and can be considered as a local defect in the polymer structure. Notice that the mechanisms outlined before simply lead to the formation of hydrogen rich and hydrogen poor species or segments of these species present in the same chain, by catalyzed hydrogen transfer occurring already at room temperature.

As mentioned before, the oligomerization reactions and the side reactions III and IV of Scheme 3 proceed simultaneously.

SCHEME 4: Ring Opening Reaction with the Formation of γ-Diketone Structures

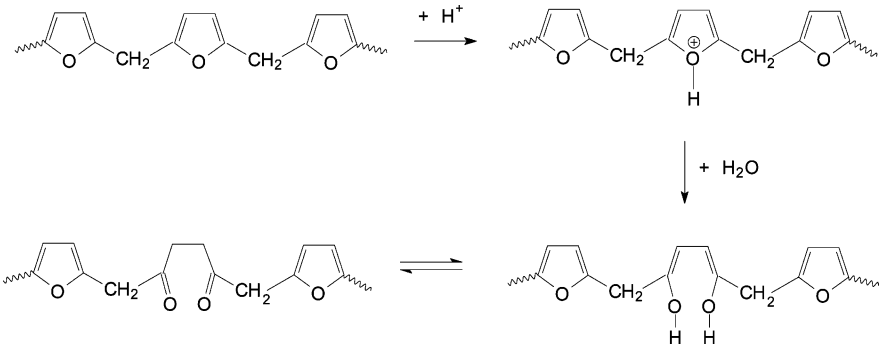

SCHEME 5: Simplified Scheme of Carbon Formation

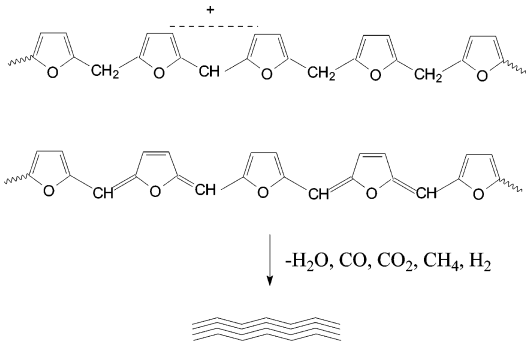

This fact explains why the color appears immediately during the oligomerization and why the intensity becomes very high already at room temperature.

Gandini et al.[17] have given strength to the mechanism of the formation of colored species by investigating the UV−vis spectroscopy of a series of model carbenium ions containing an increasing number of conjugated bonds. However, any attempt to follow the formation of the carbenium species, directly on the reacting sample, is made difficult by the fact that the reaction is fast and that many types of species are formed nearly simultaneously.

When the viscous (and colored) material is subjected to thermal treatment in a flow of inert gas by gradually increasing the temperature from 300 to 1000 K, the material becomes rigid and black, due to the process of carbonization, leading finally to the formation of amorphous carbon. During this process, water and other gases are released. Whether this process is also (at least partially) acid catalyzed is not known. A plausible scheme of carbon formation is illustrated in Scheme 5.

This scheme is oversimplified, since it does not consider the methyl terminated chains (see Scheme 2) and the species illustrated in Scheme 4. Furthermore, the formation of branched species, whose presence has been demonstrated by NMR[18] and thermal analysis,[19] has been ignored.

In order to better understand the mechanism of formation and the structure of colored products formed during the oligomerization at 300 K, we have decided to study the acid-catalyzed resinification of furfuryl alcohol in the restricted spaces present in the framework of a protonic Y zeolite (Si/Al = 2.6), which is populated by strong Brønsted sites (about three sites per cavity) which can act as efficient catalytic centers for oligomerization and generation of colored species. H−Y zeolite has a faujasitic type structure characterized by the simultaneous presence of large (supercages) and small (sodalite cages) internal cavities. The three-dimensional framework is generated by connecting sodalite units through hexagonal prisms to give a structure characterized by supercages with a diameter of about 13 Å.[20] The supercages are interconnected by openings of about 8 Å diameter.

The basic idea is that restricted spaces of the supercages can impose a constraint to the growth of the oligomeric chains and that this fact could also moderate the formation of conjugated sequences responsible for the color. In this way, it could be possible to follow the formation of the individual colored species and, hence, to allow a detailed study of their structure via in situ UV−vis, Fourier transform infrared (FTIR), and Raman spectroscopies, under controlled atmosphere.

An analogous study concerning the formation of cationic species by HCl-catalyzed condensation of furfuryl alcohol, during a sol−gel process of tetraethoxylane (TEOS) hydrolysis in water, has been performed by Müller et al.[12] This study has some similarities with the present one because in both cases the cationic species are formed in restricted spaces. The solid matrices and catalysts are however quite different.

As the spectroscopic methods can be applied to samples contacted with furfuryl alcohol in a large temperature interval (from 300 to 673 K), a series of experiments has been planned to follow not only the first oligomerization stages (where the formation of short conjugated double bonds sequences is supposed to occur) but also the formation of more complex products associated with longer conjugated sequences. Furthermore, for temperatures near 673 K, this methodology could also give information on the incipient carbonization process, which is leading to the formation of a carbonaceous replica phase inside the internal porosity of the zeolite.[7−9,21,22]

2. Experimental Methods

The materials used in this work were prepared starting from commercial NH_4−Y (Zeolyst CBV 500, Si/Al = 2.6). This zeolite contains sodium (Na_2O 0.2 wt %) and hence should be more properly considered as NH_4−Na−Y.

Before adsorption of furfuryl alcohol (FA) (Aldrich), the zeolite samples were activated by outgassing at 673 K for 1 h under dynamic vacuum (residual pressure: 10^{-4} mbar), to transform them into the parent protonic form. In order to obtain samples nearly free from carbonaceous adsorbed impurities at the end of the activation period in vacuo, 40 mbar of oxygen was dosed (still at 673 K) for 1 h. Only after this treatment, the sample was outgassed up to a final pressure of 10^{-4} mbar at the same temperature. Finally, the sample was cooled to room temperature (RT) under dynamic vacuum before in situ FA dosage from the gas phase. For Raman analysis, the treatment in oxygen at 673 K is not sufficient to eliminate all the carbonaceous species, which are strongly luminescent. In this

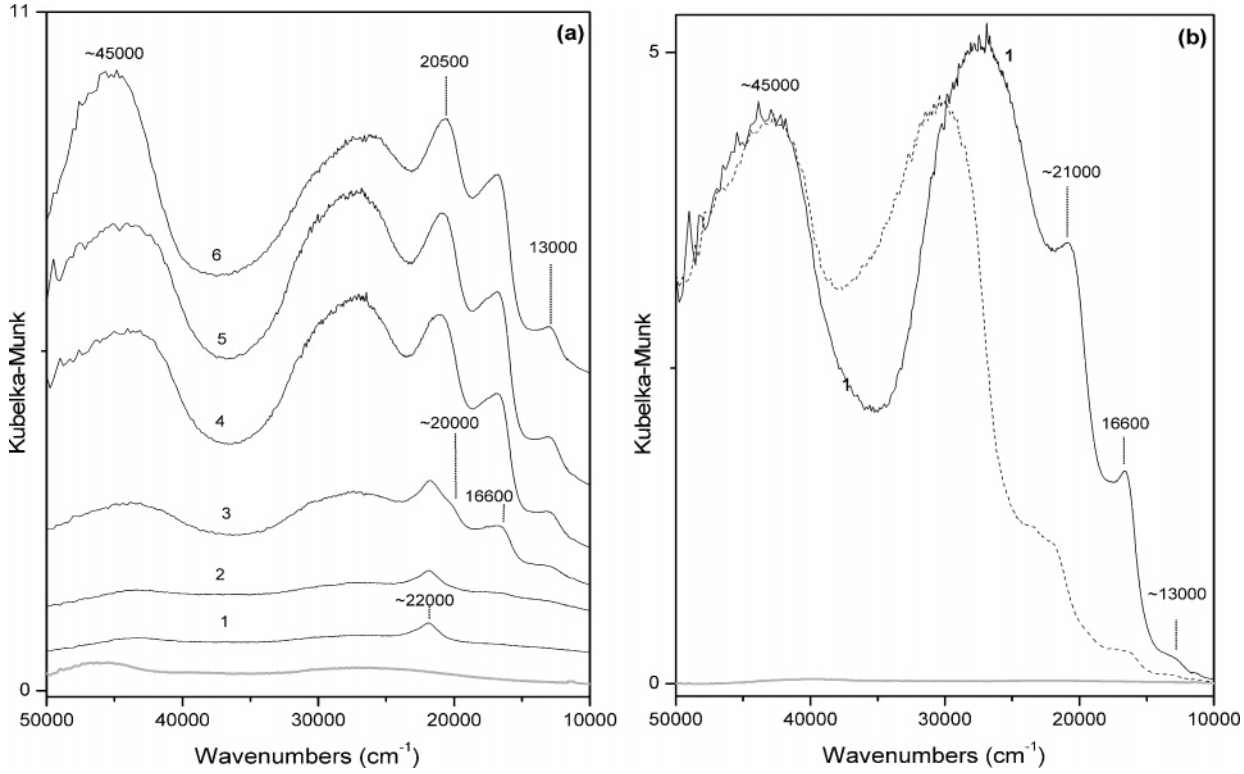

Figure 1. (a) UV−visible spectra of increasing doses of FA adsorbed on H−Y zeolite at 300 K (curves 1−5). Curve 6 has been collected in FA atmosphere for 1 h at 300 K. (b) UV−visible spectra of FA adsorbed on H−Y zeolite at 300 K before (curve 1) and after contact with NH_3 at 300 K ($p(NH_3) = 85$ mbar) (dashed line). Gray lines report the spectra of H−Y outgassed at 673 K before FA dosage.

case, the temperature of treatment in oxygen was increased to 773 K before outgassing under vacuum and cooling at RT. All activation treatments were performed in the same cells used for the spectroscopic measurements. FA was dosed from the gas phase by means of a vacuum line permanently attached to the measurement cells.

Raman spectra have been recorded at RT under controlled atmosphere by using a Renishaw micro-Raman System 1000 spectrometer (objective 20×) and a He−Cd laser emitting at 442 nm. Diffuse reflectance UV−visible spectra were recorded directly on the powdered material at RT by means of a Perkin-Elmer spectrometer (UV−vis Lambda19) equipped with a diffuse reflectance attachment.

For FTIR experiments, thin, self-supported pellets of zeolite powder were used. The IR measurements were carried out, at 2 cm^{-1} resolution, using an IFS 28 Bruker Fourier transform spectrometer (equipped with cryogenic MCT detector).

2.1. Computational Methods. In order to calculate the vibrational frequencies of model carbocationic species similar to those reported in Scheme 3 (structure I), a simplified structure was adopted, including only two furan cycles and the central −CH− linkage. As the formed carbocations in the zeolite matrix are interacting with the negative charged framework, a more realistic model including a Cl^- counterion (simulating the negative zeolite framework) has been adopted.

Calculations have been performed at the B3-LYP[23,24] level adopting a standard 6-31+G** Gaussian basis set and the Gaussian 03 software package.[25] Calculations on bare carbocation have been performed adopting a +1 charge. For the carbocation−Cl^- system, no charge has been imposed during calculations. The frequencies, and the correspondent IR spectra, have been obtained on the fully optimized structures (point group symmetry C_{2v}). Computed frequencies have been scaled by a factor of 0.9652, as suggested for furane at the above specified level of theory.

3. Results and Discussion

3.1. UV−Visible Spectra. In Figure 1a, the UV−visible spectra of increasing doses of FA adsorbed on H−Y zeolite at 300 K are reported (curves 1−6). In this figure, the spectrum of the H−Y outgassed at 673 K before FA dosage is also reported (gray line).

From this sequence of spectra, the following can be observed:

(i) The presence of a high intensity broad band at ∼45000 cm^{-1}, which can be attributed to unreacted furfuryl alcohol (either hydrogen bonded to protonic sites or simply physically adsorbed on walls). This feature is substantially identical to that obtained in solution, which shows a peak maximum at 218 nm (∼45870 cm^{-1}) and it is due to the $\pi-\pi^*$ transition of the furan ring.[26,27]

(ii) A second broad band is observed at ∼29500−25000 cm^{-1} (curves 1−2), whose intensity increases gradually with the increase of the FA dosage (curves 3−5) up to the saturation pressure of FA (curve 6). This broad band is a composite, as shown by its asymmetric character and by the presence (at the lowest coverages) of a clear shoulder at about 31000−32000 cm^{-1}. We believe that many species (positively charged and neutral: vide infra) are simultaneously contributing.

(iii) Narrower bands are observed at ∼22000−20000, 16600, and 13000 cm^{-1}. These bands show a different behavior upon FA dosage, as the 22000 cm^{-1} is the first to grow up.

These spectral features are undoubtedly due to sequences of conjugated double bonds, as also demonstrated in a recent study by means of fluorescence microscopy.[28] Whether they belong to neutral or cationic species is not possible to infer from Figure 1a.

Spange et al.[29] have reported a similar sequence of UV−vis spectra for a polyfurfuryl alcohol (PFA)−amorphous silica (aerosil) composite before and after successive addition of pyridine. They have been able to support the existence of an

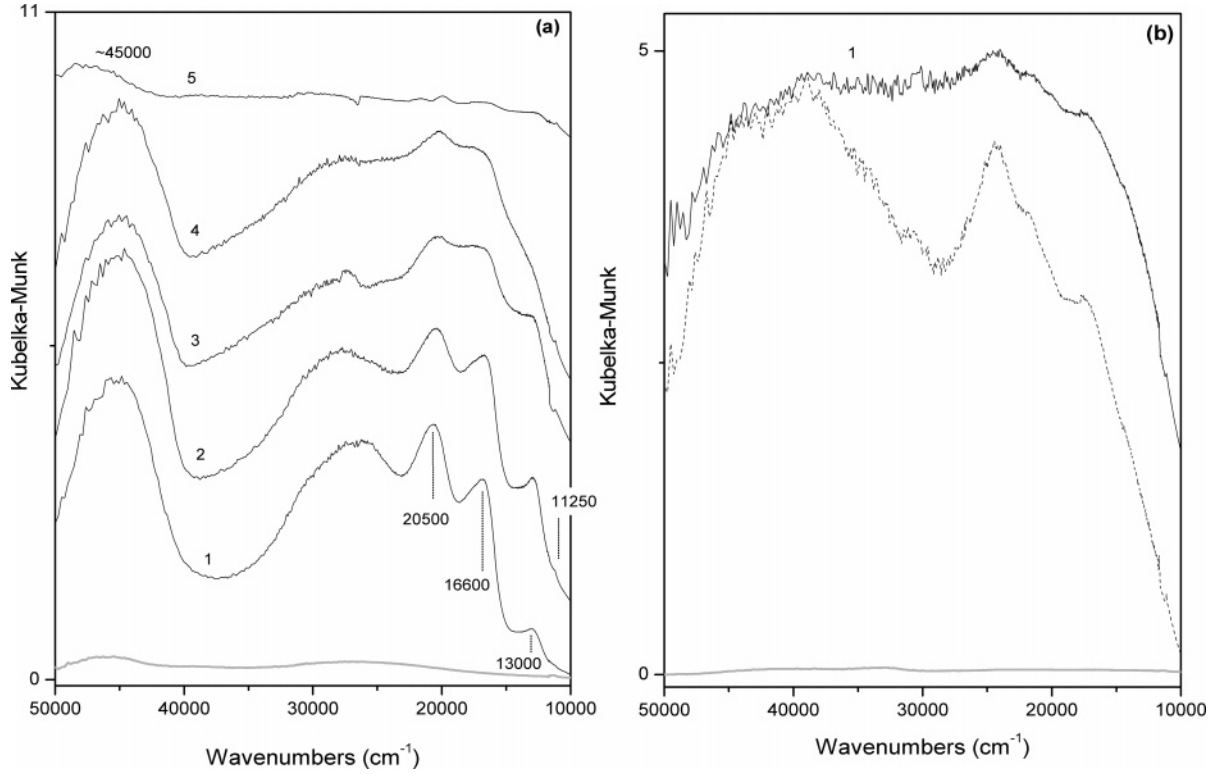

Figure 2. (a) UV−visible spectra of FA adsorbed on H−Y zeolite at 300 (curve 1), 323 (curve 2), 433 (curve 3), 573 (curve 4), and 673 K (curve 5) for 1 h. (b) UV−visible spectra of FA adsorbed on H−Y zeolite at 573 K before (curve 1) and after contact with NH_3 at 300 K ($p(NH_3) = 200$ mbar) (dashed line). Gray lines report the spectra of H−Y outgassed at 673 K before FA dosage.

equilibrium between the neutral conjugated species, formed by FA polycondensation, and the cationic species derived from protonation with HCl.

By following a similar approach (whose validity has already been verified for cationic species formed upon oligomerization of acetylenic compounds in acidic zeolite channels),[31] the effect of NH_3 dosage has been studied and the results are reported in Figure 1b. In fact, only cationic species are expected to be neutralized by the interaction with a base, because they are transformed into neutral species.[17,27,30,31]

The results shown in Figure 1b clearly show that, while the band at 45000 cm^{-1} is unaltered, all the remaining bands in the 29000−13000 cm^{-1} interval are affected by the interaction with NH_3.

From this, it can be concluded that:

(i) The attribution of the 45000 cm^{-1} band to a $\pi-\pi^*$ transition of a neutral monomeric species is confirmed.

(ii) The bands at 29000, 22000, 16600, and 13000 cm^{-1} are due to double bond sequences in cation carbenium species.[29]

As for the 29000 cm^{-1} band, we think that also neutral species of the type of structure IV, formed during the process depicted in Scheme 3, are contributing.

The most obvious assignment of the bands perturbed by NH_3 adsorption can be made on the basis of structures I and III depicted in Scheme 3, which contain an increasing number of conjugated double bonds in carbenium type sequences.

As the band at 29000 cm^{-1} is the most intense of the spectrum, it is inferred that at 300 K the most abundant cationic species are containing the simple sequence

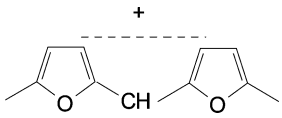

and that more complex sequences are playing a minor role.

This conclusion indicates that the chosen strategy to grow the oligomeric species in the restricted space, represented by the zeolite supercages, is correct. The reaction with NH_3 is transforming the positively charged and highly colored oligomers into "optically silent" neutral species and via the formation of adducts with NH_3, which is an electron donating system. These species are absorbing at higher frequency and (more importantly) are characterized by lower extinction coefficients.[30] We have chosen the NH_3 molecule because it is sufficiently small to diffuse into the channels even in the presence of entrapped oligomeric species.

Notice that after NH_3 adsorption a new broad band appears at 31000−32000 cm^{-1}. We believe that this broad band corresponds to the formation of the neutral species. These neutral species are only partially derived from neutralization of the cationic ones and their absorption band is superimposed to that of preexisting neutral species (see for instance the species illustrated in Scheme 4).

To verify whether the interpretation advanced before is reasonable, we have studied also the formation of colored species at temperatures higher than 300 K. This experiment has been suggested by the obvious hypothesis that oligomerization at higher T can lead to an increase of the length of the oligomers and hence also of the length of cationic species. This means that, upon increasing T, the bands in the lowest frequency interval, associated with longer sequences of conjugated double bonds in cationic species, should show a preferential growth.

In Figure 2a, we report the results of an experiment where the temperature has been increased gradually from 300 K (curve 1) to 673 K (curve 5). The gray line represents the UV−vis spectrum of H−Y outgassed at 673 K before FA dosage.

From this figure, it is evident that (i) heating in the 300−573 K range leads to an effective intensification of the bands at 20500, 16600, and 13000 cm^{-1}, as expected; (ii) a new weak peak can be observed at 11250 cm^{-1}; (iii) the bands in the

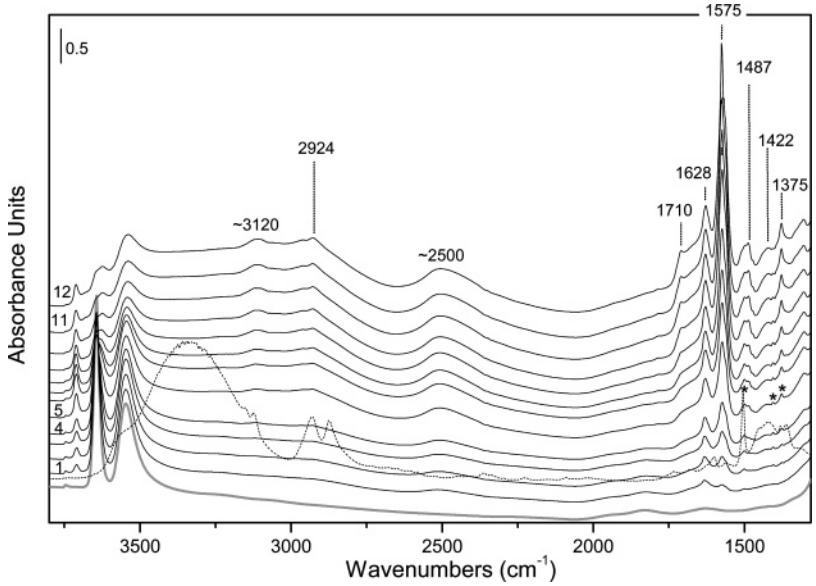

Figure 3. FTIR spectra of increasing doses of FA adsorbed on H−Y zeolite at 300 K (curves 1−11). Spectrum 12 has been collected in FA atmosphere for 1 h at 300 K (p(FA) = 0.6 mbar). The dotted line reports the spectrum of liquid FA at 300 K, and the gray line reports the spectrum of H−Y outgassed at 673 K before FA dosage.

20500−13000 cm^{-1} range tend to coalesce and, at 673 K, they form a broad envelope where the single components can be singled out with difficulty; (iv) the band at 45000 cm^{-1} remains unchanged until 573 K; (v) the absorption in the 25000−30000 cm^{-1} range is apparently unchanged in the 300−433 K interval; (vi) the sample treated at 673 K is "black" in the whole 50000−15000 cm^{-1} interval. The corresponding featureless spectrum certainly is due to the extensive formation of amorphous carbon.

To verify the contribution of neutral and cationic species to the spectral features illustrated in Figure 2a, the effect of NH_3 dosage at 300 K on a FA/H−Y system treated at 573 K has been studied, and the result is reported in Figure 2b. From this, it is possible to conclude that (i) the bands associated with carbocationic species are strongly weakened because of the neutralization effect of NH_3 and (ii) a weaker and complex spectrum remains, which is assigned to the neutral oligomers either generated by the neutralization effect or formed by the reaction depicted in Scheme 4. Notice that the maximum is shifted now to 25000−20000 cm^{-1}, which is a frequency interval definitely lower than that observed in Figure 1b. This corresponds to the fact that the neutral oligomers are characterized by longer chains, containing a number of conjugated double bonds peaking at about seven.[31,32]

All of these results, together with the experiments reported before in Figure 1b and with the literature data concerning FA polymerization,[15,17] prove the carbocationic character of the species formed in the zeolite channels upon proton attack. On the other hand, the UV−vis experiments presented so far are not sufficient to determine the correct structures of the carbocationic species because optical transitions give only correct information on the number of conjugated double bonds. Further confirmation by means of other spectroscopic techniques, such as IR and Raman, is consequently needed. For this purpose, the subject of the second part of the contribution will deal with them.

3.2. FTIR and Raman Spectra. Before illustrating and discussing the IR data concerning the FA adsorption on H−Y zeolite, it can be useful to recall the spectroscopy of the acidic O−H groups of the faujasitic structure.[33] The absorption at ∼3640 cm^{-1} (high frequency band, HF), characteristic of H−Y activated in vacuo at 673 K, is the ν(OH) of Brønsted groups protruding in the supercages, while the absorption at 3550 cm^{-1} (low frequency band, LF) is the ν(OH) of Brønsted groups located in the sodalite units.[34,35]

Figure 3 shows the IR spectra of FA adsorbed on H−Y zeolite at 300 K. In this figure, the first curve represents the IR spectrum of H−Y outgassed at 673 K before FA dosage. In this spectrum, we also notice a very weak feature at 3746 cm^{-1}, which is due to the ν(O−H) stretching of the Si−OH groups on the external faces of the zeolite crystals.[34,35] Its very low intensity is due to the low external surface area of the H−Y microcrystals.

Spectra 1−11 have been registered after contact of increasing doses of FA at 300 K, while spectrum 12 has been obtained after contact with a FA atmosphere for 1 h at 300 K (p(FA) = 0.6 mbar). The spectrum of pure liquid FA, recorded at 300 K, is also reported (dotted line).

From this sequence of spectra, it is clearly inferred that increasing doses of FA at 300 K are associated with a decrease of the intensity of the HF band at 3643 cm^{-1}, up to complete disappearance at highest dosages (curve 12). This indicates that FA interacts with the Si−OH−Al species in the supercages. At the highest dosages, a slight decrease in intensity and broadening is also observed for the LF band at 3547 cm^{-1}, which means that filling the supercages with FA also partially affects Brønsted acid sites located in the sodalite units.

The decrement of the band at 3643 cm^{-1} is accompanied by the parallel growth of a broad and complex absorption in the ∼3300−1800 cm^{-1} range, which can be interpreted on the basis of the formation of strongly hydrogen-bonded species (OH⋯FA) between the Brønsted groups and FA in the supercages. In particular, the components at ∼2800, ∼2500, and 1800 cm^{-1} are ascribed to the characteristic ABC triad caused by Fermi resonance of the broad ν stretching mode with 2δ and 2γ overtones.[36]

Besides the broad band due to ν (OH⋯FA), the CH stretching vibrations of hydrogen-bonded FA are observed at ∼3120 and 2924 cm^{-1}. Besides the above-mentioned spectroscopic manifestations, many components at 1710, 1628, 1575, 1510, 1487, 1422, and 1375 cm^{-1} are also growing with the coverage and with the contact time (curves 1−12).

These bands have different coverage and time dependence with respect to those described before. In particular, the peak

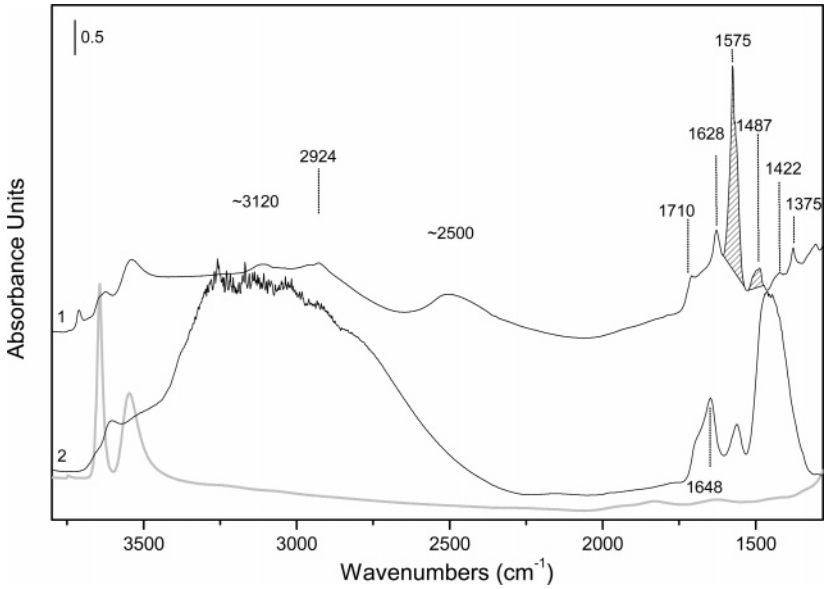

Figure 4. FTIR spectra of FA adsorbed on H−Y zeolite at 300 K for 1 h (curve 1) and after contact with NH_3 on FA precovered H−Y zeolite at 300 K (curve 2). (p(FA) = 0.6 mbar and p(NH_3) = 1 mbar). Gray line reports the spectrum of H−Y outgassed at 673 K before FA dosage.

at 1575 cm^{-1} becomes predominant at the highest contact time. About the detailed assignment of the bands, the following should be mentioned:

(i) The very weak bands at 1510, 1422, and 1375 cm^{-1}, clearly observed only at lowest dosage, are due to molecularly adsorbed FA because they correspond with the peaks of FA liquid (dotted spectrum, asterisks on curve 4).[37] These bands are no longer observable at the highest dosages because they become overshadowed by the oligomerization products.

(ii) The band at 1710 cm^{-1} can be attributed to the stretching vibration of a carbonyl species. This assignment supports the hypothesis that, during oligomerization, formation of diketonic structures is occurring, following Scheme 4.[15,38]

(iii) The band at 1628 cm^{-1} is of problematic assignment. In fact, it could be ascribed to the bending mode of H_2O coordinated to the sodium cations of the H−Y zeolite[39] (H_2O molecules are formed during the condensation processes, as reported in Schemes 1 and 2) or to the ring stretching mode of the 2,3-bisubstituted furan rings, as suggested in ref 40, thus supporting the formation of branched species.[18,19] As this band is observed also after heating at 433 K (vide infra: Figure 6, that is, after treatment conditions ensuring water desorption), we think that the second attribution is more convincing.

(iv) Significant absorptions are observed at 1575 and 1487 cm^{-1}. These bands are attributed to the ν(C═C) modes of neutral or cationic polyunsaturated species.[31] We shall return to this point in the following, when we illustrate the effect of NH_3 dosage, which destroys the carbocationic species, as already known on the basis of the UV−vis results.

In Figure 4, the effect of NH_3 dosage at 300 K on preadsorbed FA is illustrated. From this figure, it is clearly emerging that the bands at 1575 and 1487 cm^{-1} are completely eroded upon NH_3 contact. Simultaneously, new components in the 3400−2400 cm^{-1} interval, at 1648 and at 1470−1440 cm^{-1}, increase (curve 2). Also the complex absorption ascribed to hydrogen-bonded species (3500−2000 cm^{-1} range, vide supra) disappears, because the acid sites are neutralized by the interaction with NH_3 with promotion of NH_4^+ groups and hence the OH···FA hydrogen-bonded species are destroyed.

From this, the following can be concluded: The bands at 1575 and 1487 cm^{-1} are due to carbocationic oligomeric species (filled areas under curve 1). On the basis of purely experimental data, it is not easy to assign the two bands to specific modes of the cationic species. Great help is coming from computer simulation of the vibrational frequencies performed on the model structures

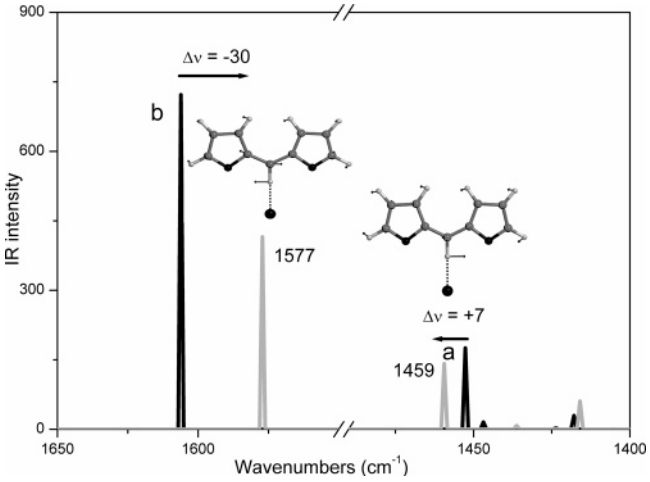

Figure 5. Computed IR spectra in the 1650−1400 cm^{-1} region of a bare cationic model species (black line) and of the same species interacting with Cl^- (gray line). In the same figure, pictorial representations of vibrational modes (atomic displacements indicated by black arrows) associated with bands a and b in the spectrum are reported. White spheres, H atoms; gray spheres, C atoms; small black spheres, O atoms; large black spheres, Cl atoms.

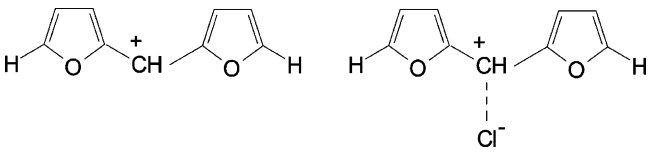

which are simulating the relevant moieties of the carbocationic species. The results concerning the modes with frequencies in the 1650−1400 cm^{-1} interval (i.e., the modes having prevalently ν(C═C) stretching character and presumably not very much influenced by the model character of the structure) are illustrated in Figure 5. We can see that the correspondence between the calculated and observed frequencies, and their intensities, is very good (especially when the cation−anion pair is considered).

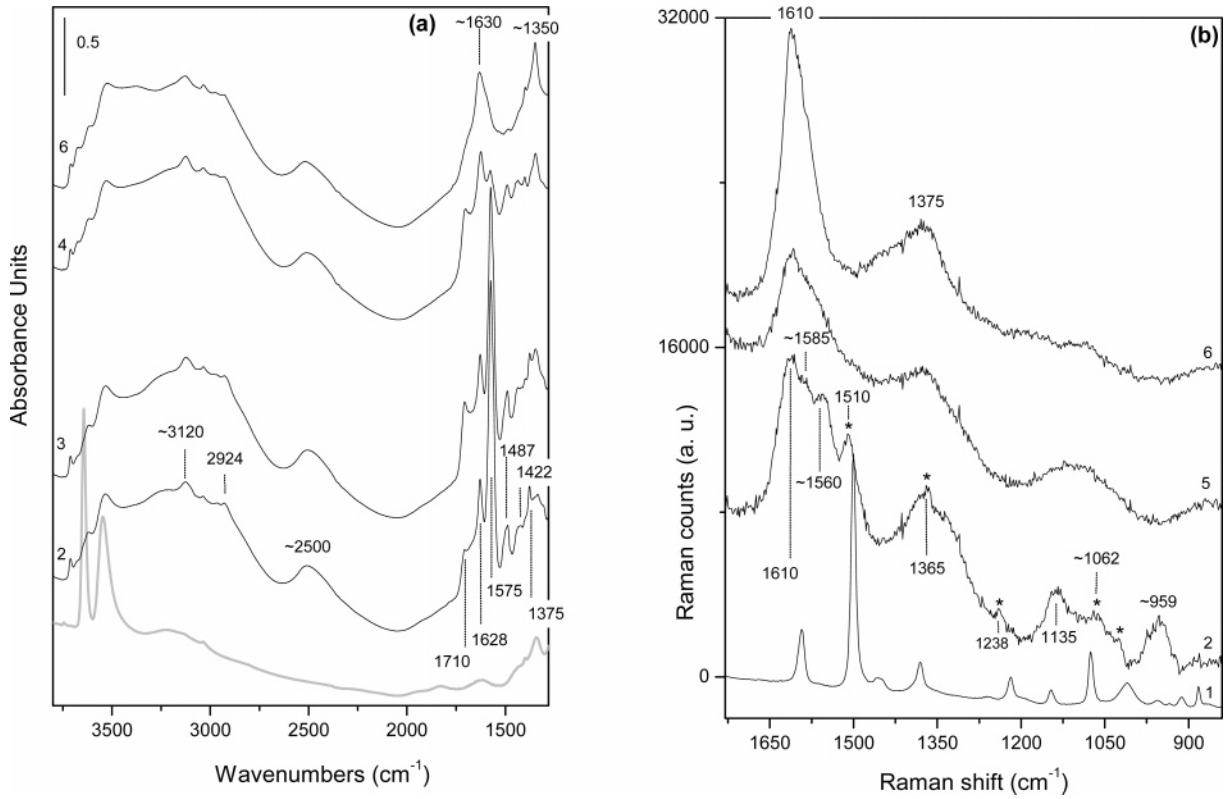

Figure 6. (a) FTIR spectra of FA adsorbed on H−Y zeolite at 300 (curve 2), 323 (curve 3), 433 (curve 4), and 673 K (curve 6) for 1 h (p(FA) = 0.6 mbar). The gray line reports the spectrum of H−Y outgassed at 673 K before FA dosage. (b) Raman spectra of FA adsorbed on H−Y zeolite at 300 (curve 2), 573 (curve 5), and 673 K (curve 6) for 1 h (at 442 nm laser excitation-400*10, 1% power) (p(FA) = 1 mbar). Curve 1 reports the spectrum of liquid FA at 300 K.

This result is relevant not only because it allows a detailed assignment, but also because it demonstrates that the oligomerization in restricted spaces allows one to clearly observe, for the first time, the vibrational modes of distinct cationic species.

The broad and complex absorption in the range 3400−2400 cm^{-1} is due to the ν(NH) modes of hydrogen-bonded $[NH_4]^+$, while the bands at 1648 and 1470−1440 cm^{-1} are due to $\delta(NH_4)^+_n$ modes of the same species.[41]

In order to understand whether longer oligomers can also be formed under different conditions and fill the internal voids, new IR and Raman experiments at temperatures higher than 300 K have been performed.

In particular, in Figure 6a, the IR spectra of FA adsorbed on H−Y zeolite at temperatures ranging from 300 up to 673 K are reported. Spectrum 2 has been collected in the presence of FA atmosphere at 300 K after 1 h (p(FA) = 0.6 mbar), while spectra 3, 4, and 6 have been registered after treatment in FA atmosphere at 323, 433, and 673 K for 1 h, respectively. The gray spectrum corresponds to H−Y outgassed at 673 K before FA dosage.

From this figure, the following is evident:

(i) Heating in the 300−323 K range (curves 2 and 3) does not substantially affect the IR absorptions.

(ii) The bands at 1710 and 1628 cm^{-1} remain unchanged until 433 K, while at this temperature the components at 1575 and 1487 cm^{-1} start to decrease in intensities.

(iii) The absorptions in the 3800−2400 cm^{-1} range are apparently unaffected by thermal treatments until 673 K.

(iv) On the sample treated at 673 K, two main and broader bands at ∼1630 and ∼1350 cm^{-1} become dominating (with shoulders at ∼1700 and ∼1580 cm^{-1}). At the same time, the bands at 1710, 1628, 1575, 1487, 1422, and 1375 cm^{-1} are completely eroded. On the basis of the literature data concerning amorphous carbon and single-walled and multiwalled carbon nanotubes (MWCNTs and SWCNTs),[42−44] absorptions at ∼1630 and ∼1350 cm^{-1} indicate the initiation of the carbonization process of the FA oligomers.

These results also indicate that the transformation of the oligomeric species into neutral carbonaceous chains is already initiating at 433 K. Whether these species are internal or external, we shall return to this topic in the following.

In order to better understand the nature of the formed species, the same experiment has been done by means of in situ Raman spectroscopy.

In Figure 6b, Raman spectra of FA adsorbed on H−Y zeolite at temperatures ranging from 300 up to 673 K are reported. In particular, spectrum 2 has been collected in the presence of FA atmosphere at 300 K after 1 h (p(FA) = 1 mbar), while spectra 5 and 6 have been registered after treatment in FA atmosphere at 573 and 673 K for 1 h, respectively. The spectrum of pure liquid FA, collected at 300 K, is also reported (curve 1).

The exciting line (λ = 442 nm, corresponding to 22624 cm^{-1}) is expected to be able to induce the Raman resonant effect on species adsorbing in the visible region. As discussed before, in this range, both neutral and cationic conjugated species are absorbing: consequently, we expect the Raman spectrum is dominated by the vibrational manifestations of them.

Concerning the micro-Raman spectrum taken at 300 K, it must be emphasized that the part exposed to the beam is lightly darkening, even when the lowest power is used. This means that the local temperature is higher than 300 K. This implies that, under the laser beam, the samples exposed to FA at 300 K can already contain species that are characteristic of samples treated at higher temperatures. On the basis of this observation

and of the frequency of the exciting line, we shall hereafter assume that the observed spectrum corresponds to a mixture of cationic, oligomeric, and carbonaceous species.

Coming to the Raman spectra of Figure 6, the following features should be mentioned:

(i) When FA is adsorbed on H−Y at 300 K for 1 h (curve 2), many features are observable in the 1700−900 cm^{-1} range. We think that the bands at 1510, 1365, 1238, ∼1062, and ∼1024 cm^{-1} (asterisks on curve 2) are due to the vibrational modes of chains of PFA, because they are very similar to those of liquid FA (curve 1). On the contrary, the peaks at ∼1585, ∼1560, 1135, and ∼959 cm^{-1} are assigned to cationic unsaturated moieties inserted into the polymeric chains (see Scheme 3, structures I and III). Most likely, these peaks are the vibrational counterparts of the 26000−20000 cm^{-1} bands observed in the UV−vis spectrum. These bands are superimposing to broader absorptions centered at 1610 and 1375 cm^{-1}, which are characteristic of amorphous carbon (G and D peaks).[40,45,46] The contemporary presence of all of these features, already at 300 K, reveals the coexistence, under the laser beam, of both molecular-type cationic and neutral (carbon-type) species. Whether the early formation of species, characteristic of an advanced state of resinification, is due to the local heating effect of the laser beam or to a photocatalyzed process is difficult to ascertain.

The previous attributions are confirmed by the spectra obtained heating at 573 K (curve 5) and at 673 K (curve 6). In fact, all of the features ascribed to molecular-type oligomeric and cationic species progressively disappear, while the complex absorptions due to amorphous carbon gradually increase and become predominant. This means that complete transformation of the FA polymer into a disordered carbon is occurring both in the H−Y channels, progressively filling the internal voids, and on the external zeolite surface.

4. Conclusions

The acid-catalyzed oligomerization and resinification of furfuryl alcohol in the cavities of H−Y zeolite have been followed by means of FTIR, Raman, and UV−vis spectroscopies. The reduced speed of the reaction, induced by the restricted spaces, has allowed many intermediates formed during the initial stage of polymerization to be characterized. The vibrational assignments of the modes of carbocationic species have been confirmed by computer simulations on model compounds. The carbocationic character of the species formed inside the zeolite channels, upon proton attack on furfuryl alcohol, has been demonstrated clearly by dosing NH_3, which preferentially affects the spectra of the charged species.

The UV−vis, FTIR, and Raman results, obtained after oligomerization at temperatures higher than 300 K, show that the length of the oligomers and of the cationic species increases with increasing temperature. Finally, it is shown that, on samples treated at 673 K, the formation of amorphous carbon on H−Y zeolite is clearly observable. This carbonaceous material is gradually filling the internal pores, and contemporarily, it is forming on the external surface. The formation of the carbonaceous material can occur at lower temperature under the action of a laser line at 22624 cm^{-1}.

Acknowledgment. This work was supported by MIUR (Ministero dell'Istruzione, dell'Università e della Ricerca), INSTM Consorzio, Centre of Reference INSTM (Torino), and NIS (Nanostructured Interfaces and Surface) Centre of Excellence. The authors acknowledge financial support by Regione Piemonte (Progetto NANOMAT, Docup 2000−2006, Linea 2.4a).

References and Notes

(1) Dunlop, A. P.; Peters, F. N. *The Furans*; Reinhold Publishing Co.: New York, 1953.

(2) Schmitt, C. R. *Polym.-Plast. Technol. Eng.* **1974**, *3*, 121.

(3) Killip, W. J.; Sherman, E. *Furan Derivatives*; In *Kirk-Othmer Encyclopedia of Chemical Technology*; Grayson, M., Ed.; John Wiley & Sons: New York, 1981; Vol. 11, pp 499−527.

(4) Leitheiser, R. H.; Londrigan, M. E.; Rude, C. A. In *Plastics Mortars, Sealants and Caulking Compounds*; Seymour, R. B., Ed.; ACS Symposium Series No. 113; American Chemical Society: Washington, DC, 1979; p 7.

(5) Kyotani, T. *Carbon* **2000**, *38*, 269−286.

(6) Ma, Z.; Kyotani, T.; Tomita, A. *Chem. Commun.* **2000**, 2365−2366.

(7) Ma, Z.; Kyotani, T.; Tomita, A. *Carbon* **2002**, *40*, 2367−2374.

(8) Hou, P.-X.; Orikasa, H.; Yamazaki, T.; Matsuoka, K.; Tomita, A.; Setoyama, N.; Fukushima, Y.; Kyotani, T. *Chem. Mater.* **2005**, *17*, 5187−5193.

(9) Barata-Rodrigues, P. M.; Mays, T. J.; Moggridge, G. D. *Carbon* **2003**, *41*, 2231−2246.

(10) Uota, M.; Yada, M.; Kuroki, M.; Machida, M.; Kijima, T. *Carbon* **2004**, *42*, 2207−2213.

(11) Meyers, C. J.; Shah, S. D.; Patel, S. C.; Sneeringer, R. M.; Bessel, C. A.; Dollahon, N. R.; Leising, R. A.; Takeuchi, E. S. *J. Phys. Chem. B* **2001**, *105*, 2143−2152.

(12) Müller, H.; Rehak, P.; Jäger, C.; Hartmann, J.; Meyer, N.; Spange, S. *Adv. Mater.* **2000**, *12* (22), 1671−1675.

(13) Wewerka, E. M.; Longhran, E. D.; Waters, K. L. *J. Appl. Polym. Sci.* **1971**, *15*, 1437−1451.

(14) Wewerka, E. M. *J. Polym. Sci.* **1971**, A*19*, 2703−2715.

(15) Conley, R. T.; Metil, I. *J. Appl. Polym. Sci.* **1963**, *7*, 37−52.

(16) Maciel, G. E.; Chuang, I. S.; Myers, G. E. *Macromolecules* **1984**, *17*, 1087−1090.

(17) Choura, M.; Belgacem, N. M.; Gandini, A. *Macromolecules* **1996**, *29*, 3839−3850.

(18) Principe, M.; Ortiz, P.; Martinez, R. *Polym. Int.* **1999**, *48*, 637−641.

(19) De la C. Garcia, T.; Gomez, M. R.; Martinez, R.; Alonso, C. *Polym. Int.* **2003**, *52*, 86−91.

(20) Marra, G. L.; Fitch, A. N.; Zecchina, A.; Ricchiardi, G.; Salvalaggio, M.; Bordiga, S.; Lamberti, C. *J. Phys. Chem. B* **1997**, *101*, 10653−10660.

(21) Lu, A.; Schmidt, W.; Spliethoff, B.; Schüth, F. *Adv. Mater.* **2003**, *15* (19), 1602−1606.

(22) Vergunst, Th.; Kapteijn, F.; Moulijn, J. A. *Carbon* **2002**, *40*, 1891−1902.

(23) Becke, A. D. *J. Chem. Phys.* **1993**, *98*, 5648−5652.

(24) Lee, C.; Yang, W.; Parr, R. G. *Phys. Rev. B* **1988**, *37*, 785−789.

(25) Frisch, M. J.; Trucks, G. W.; Schlegel, H. B.; Scuseria, G. E.; Robb, M. A.; Cheeseman, J. R.; Montgomery, J. A., Jr.; Vreven, T.; Kudin, K. N.; Burant, J. C.; Millam, J. M.; Iyengar, S. S.; Tomasi, J.; Barone, V.; Mennucci, B.; Cossi, M.; Scalmani, G.; Rega, N.; Petersson, G. A.; Nakatsuji, H.; Hada, M.; Ehara, M.; Toyota, K.; Fukuda, R.; Hasegawa, J.; Ishida, M.; Nakajima, T.; Honda, Y.; Kitao, O.; Nakai, H.; Klene, M.; Li, X.; Knox, J. E.; Hratchian, H. P.; Cross, J. B.; Bakken, V.; Adamo, C.; Jaramillo, J.; Gomperts, R.; Stratmann, R. E.; Yazyev, O.; Austin, A. J.; Cammi, R.; Pomelli, C.; Ochterski, J. W.; Ayala, P. Y.; Morokuma, K.; Voth, G. A.; Salvador, P.; Dannenberg, J. J.; Zakrzewski, V. G.; Dapprich, S.; Daniels, A. D.; Strain, M. C.; Farkas, O.; Malick, D. K.; Rabuck, A. D.; Raghavachari, K.; Foresman, J. B.; Ortiz, J. V.; Cui, Q.; Baboul, A. G.; Clifford, S.; Cioslowski, J.; Stefanov, B. B.; Liu, G.; Liashenko, A.; Piskorz, P.; Komaromi, I.; Martin, R. L.; Fox, D. J.; Keith, T.; Al-Laham, M. A.; Peng, C. Y.; Nanayakkara, A.; Challacombe, M.; Gill, P. M. W.; Johnson, B.; Chen, W.; Wong, M. W.; Gonzalez, C.; Pople, J. A. *Gaussian 03*, revision C.02; Gaussian, Inc.: Wallingford, CT, 2004.

(26) Giuliani, A.; Walker, I. C.; Delwiche, J.; Hoffmann, S. V.; Limao-Vieira, P.; Mason, N. J.; Heyne, B.; Hoebeke, M.; Hubin-Franskin, M.-J. *J. Chem. Phys.* **2003**, *119*, 7282−7288.

(27) Spoto, G.; Geobaldo, F.; Bordiga, S.; Lamberti, C.; Scarano, D.; Zecchina, A. *Top. Catal.* **1999**, *8*, 279−292.

(28) Roeffaers, M. B. J.; Sels, B. F.; Uji.i, H.; Blanpain, B.; L'hoëst, P.; Jacobs, P. A.; De Schryver, F. C.; Hofkens, J.; de Vos, D. E. *Angew. Chem., Int. Ed.* **2007**, *46*, 1706−1709.

(29) Spange, S.; Schutz, H. *Makromol. Chem.* **1993**, *194*, 1537−1544.

(30) Bally, T.; Roth, K.; Tang, W.; Schrock, R. R.; Knoll, K.; Park, L. Y. *J. Am. Chem. Soc.* **1992**, *114*, 2440−2446.

(31) Bordiga, S.; Ricchiardi, G.; Spoto, G.; Scarano, D.; Carnelli, L.; Zecchina, A.; Otero Areàn, C. *J. Chem. Soc., Faraday Trans* **1993**, *89* (11), 1843−1855.

(32) Knoll, K.; Schrock, R. R. *J. Am. Chem. Soc.* **1989**, *111*, 7989−8004.
(33) Eichler, U.; Brändle, M.; Sauer, J. *J. Phys. Chem. B* **1997**, *101*, 10035−10050.
(34) Anderson, M. W.; Klinowski, J. *Zeolites* **1986**, *6*, 455−466.
(35) Zecchina, A.; Spoto, G.; Bordiga, S. In *Vibrational Spectroscopy of zeolites*; Chalmers, J. M., Griffiths, P. R., Eds.; Handbook of Vibrational Spectroscopy; John Wiley and Sons Ltd.: Chichester, U.K., 2002; p 3042.
(36) Zecchina, A.; Bordiga, S.; Spoto, G.; Scarano, D.; Spanò, G.; Geobaldo, F. *J. Chem. Soc., Faraday Trans.* **1996**, *92* (23), 4863−4875.
(37) Sugama, T.; Kukacka, L. E. *J. Mater. Sci.* **1982**, *17*, 2067−2076.
(38) Sugama, T.; Kukacka, L. E.; Carciello, N.; Warren, J. B. *J. Appl. Polym. Sci.* **1985**, *30*, 2137−2155.
(39) Zecchina, A.; Geobaldo, F.; Spoto, G.; Bordiga, S.; Ricchiardi, G.; Buzzoni, R.; Petrini, G. *J. Phys. Chem.* **1996**, *100*, 16584−16599.
(40) Wang, Z.; Lu, Z.; Huang, X.; Xue, R.; Chen, L. *Carbon* **1998**, *36*, 51−59.
(41) Zecchina, A.; Marchese, L.; Bordiga, S.; Pazè, C.; Gianotti, E. *J. Phys. Chem. B* **1997**, *101*, 10128−10135.
(42) Zhang, J.; Zou, H.; Qing, Q.; Yang, Y.; Li, Q.; Liu, Z.; Guo, X.; Du, Z. *J. Phys. Chem. B* **2003**, *107*, 3712−3718.
(43) Verdejo, R.; Lamoriniere, S.; Cottam, B.; Bismarck, A.; Shaffer, M. *Chem. Commun.* **2007**, 513−515.
(44) Branca, C.; Frusteri, F.; Magazù, V.; Mangione, A. *J. Phys. Chem. B* **2004**, *108*, 3469−3473.
(45) Ferrari, A. C.; Robertson, J. *Philos. Trans. R. Soc. London, Ser. A* **2004**, *362*, 2477−2481.
(46) Ferrari, A. C.; Robertson, J. *Phys. Rev. B* **2000**, *61*, 14095−14107.